THE AMERICAN MINERALOGIST, VOL. 55, MAY–JUNE, 1970

ORIGIN, MECHANISM, AND CONSEQUENCES OF COMPOSITIONAL SECTOR-ZONING IN STAUROLITE

LINCOLN S. HOLLISTER, *Department of Geological and Geophysical Sciences, Princeton University, Princeton, New Jersey 08540.*

ABSTRACT

A detailed study of the compositional variations of sector-zoned staurolite from one outcrop area and a reconnaissance study of staurolite from seventeen localities suggest that the sector-zoning phenomenon is an interrelation of chemical equilibrium between surfaces, rate of growth of the staurolite, and rates of diffusion perpendicular to the surface layers. The diffusion process is in response to a thermodynamic drive towards bulk chemical equilibrium. Strongly sector-zoned staurolite appears to occur when the growth rate exceeds the diffusion rates perpendicular to the growth layers. Weakly or nonsector-zoned staurolite appear to occur when the growth rate is about the same or slower than the diffusion rate.

The mechanism leading to the observed differences in chemistry between sectors can be understood in terms of the two-dimensional atomic configurations on the crystal faces. The coupled substitution of (3Al) for (2Si+H), leading to excess Al on the (001) face, is possible, whereas it cannot easily occur on the (010) face. The coupled substitution of (Mg+Ti) for (2Al) is easily available on the (010) face, whereas it is not so available on the (001) face.

The process leading to sector-zoning can lead to differences between the sectors in degree of order of the filled aluminum octahedra. The process also offers an insight into the mechanism of nucleation and for the development of preferred orientation of minerals in metamorphic rocks.

INTRODUCTION

The phenomenon of compositional sector-zoning in staurolite (Hollister, 1967; Hollister and Bence, 1967; Hollister, 1968; Dollase and Hollister, 1969) raises questions as to the mechanism of crystal growth in a solid medium, the relation of surface atomic arrangements to the bulk chemistry of the crystal, and the possible effects of supersaturation and rate of growth on the chemistry and crystal structure of a mineral. This paper attempts to reslove these questions by consideration of the chemical characteristics and mechanism of sector-zoning in staurolite.

For a description of compositional sector-zoning in staurolite, the reader is referred to the paper by Hollister and Bence (1967). Good descriptions of compositional sector-zoning in other minerals are given by Barton, *et al.* (1963) for minor components in sphalerite, Cohen (1960) for substitutional Al in quartz, and Hollister and Hargraves (1970) for the lunar clinopyroxenes. Briefly, compositional sector-zoning in staurolite consists of the development of distinctly different compositions behind the crystallographically distinct faces of a growing staurolite crystal. The resultant volumes of differing chemistry are roughly pyramidal in

shape, with bases at the crystal faces and with the apices coincident at the crystal center (Fig. 1). The specimen described in Hollister and Bence (1967), which came from the Kwoiek area of British Columbia (Hollister, 1969), displays the forms {110}, {010}, and {001}. The pyramids with these faces as bases are called, respectively, the (110), (010), and (001) sectors. In one crystal, there are 4 (110) sectors, 2 (010) sectors, and 2 (001) sectors. The geometry of these sectors is illustrated in Figure 1.

In this paper, compositional sector-zoning is treated as a distinct, but probably related, phenomenon from sectoral differences in inclusions (*e.g.* typical hour-glass chloritoid (Halferdahl, 1961) and adsorbed dyes). Furthermore, the chiastolite-type pattern of inclusions, frequently observed in staurolite and andalusite, probably owes its origin to the impurities (such as graphite) excluded from a growing crystal and the concentration of these impurities at the edges and corners where crystal faces meet (Penfield and Pratt, 1894). If such inclusions are present, they serve to outline boundaries of sectors; but their presence is not interpreted to be necessary for the development of compositional sector-zoning.

Four possible models are presented in this paper to account for compositional sector-zoning. They are discussed in detail, testable predictions of each model are presented, and the results of the tests are given. The data presented will support the uniqueness of a model which involves an interrelation of chemical equilibrium between surfaces, rate of growth, and rates of diffusion perpendicular to the growth layers.

The refined structure of staurolite given by Smith (1968) is used as a framework for the discussion of the chemical and structural variations of sector-zoned staurolite. It should be remembered that staurolite is unusual in that the ferromagnesian site is surrounded by four oxygen atoms rather than six as is typical in most ferromagnesian silicates. An idealized balanced formula for the unit cell of staurolite, not taking into account major reported deviations in hydrogen content, is $Fe_4^{IV}Al_{18}^{VI}Si_8^{IV}O_{48}H_2$, where the superscripts are the coordination members of the cations. Staurolite analyses also show that Mg, Ti, Zn, and Mn typically substitute into the ideal formula.

Theory

The four models discussed below were developed to include all reasonable possibilities to explain the data presented in Hollister and Bence (1967). They are not necessarily independent models but serve to emphasize each of the several factors which must be taken into account to interpret compositional sector-zoning: bulk chemical equilibrium, surface chemical equilibrium, rate of crystal growth, and poisoning of sur-

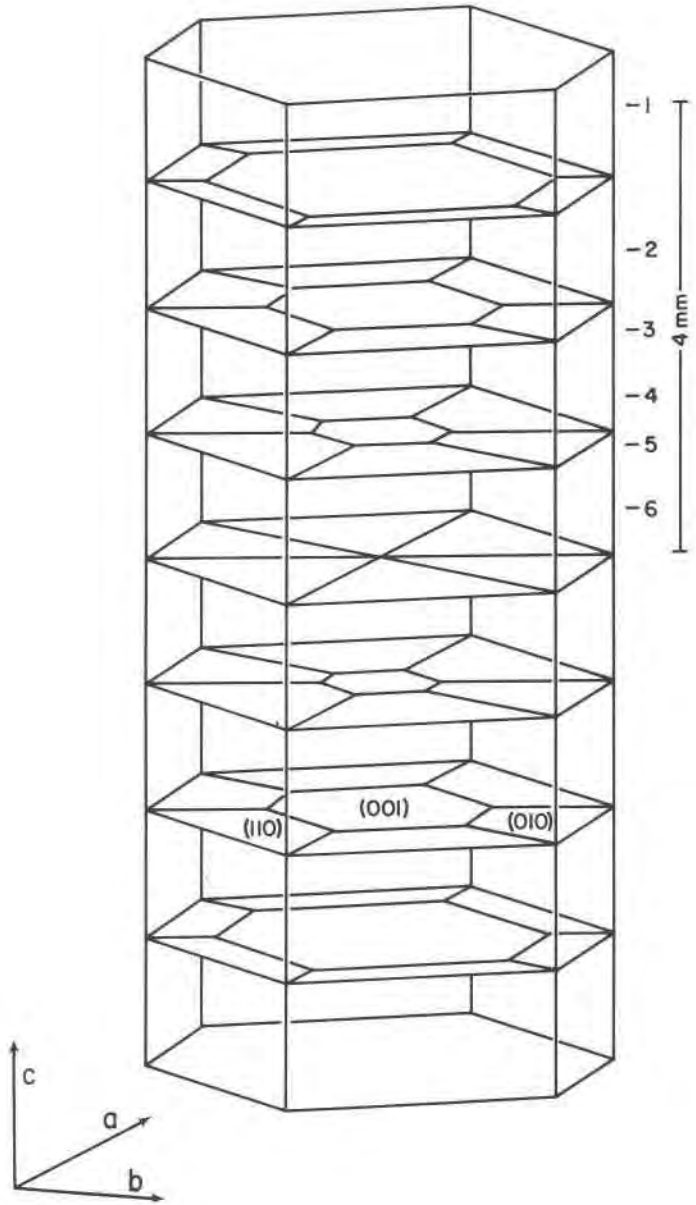

FIG. 1. Sketch showing geometry of the (001), (010), and (110) sectors in staurolite (after Harker, 1939, p. 44). Numbers 1 through 6 show relative locations of sections 350F-1 through 350F-E (Fig. 2).

faces by foreign material such as graphite. These models served to guide the collection of data.

Model I. This model considers the individual sectors of staurolite as separate thermodynamic phases, with the different compositions created at crystallographically distinct surfaces and preserved by growth. This model is similar to that used to interpret garnet zoning (Hollister, 1966) except that it postulates a unique chemistry of the growth layers for each set of distinct crystal faces irrespective of external environment and the details of crystal growth.[1] For typical garnets, all faces belong to the form {110}; for the common staurolite, there are three forms, {010}, {110}, and {001}.

The predicted consequences of this equilibrium model are (1) there will be a systematic partition of elements between any two sectors, in the same manner as between orthopyroxene and olivine (Ramberg and DeVore, 1953), and (2) all staurolite crystals with the same morphology, no matter where they occur or what the assemblage, will exhibit the sector-zoning phenomenon.

Model II. This model assumes that the sector-zoning depends only on the rate at which staurolite grew from a super-saturated environment and that the composition differences between sectors are due to differing departures from thermodynamic equilibrium. Chemical dependence on rate of growth of crystals from supersaturated solutions has been discussed by Kinsman and Holland (1969), Torgeson (1966), and McIntyre (1963). In a solid medium, the same phenomenon might be expected to depend on the chemical potential gradients of the components of staurolite in the neighborhood of the staurolite crystal. The gradients, in turn, might vary according to the distance material would have to move to the staurolite nucleus and might affect the degree of supersaturation at the growing faces.

The predicted consequences of this model are (1) the partition of elements between sectors might depend on the distance between staurolite crystals, (2) the composition of a given sector of a given crystal at any growth stage would not necessarily be the same as the composition of the same sector at the same growth stage of another crystal of the same rock, and (3) staurolite which grew slowly enough so that thermodynamic equilibrium could be established, as might be expected in a regional metamorphic terrane, would not show sectoral compositional

[1] It should be noted that there are no obvious differences in texture or phases present between the matrix adjacent to the different crystal faces in the staurolite from the Kwoiek area. The rocks typically exhibit a hornfelsic texture.

variations; but staurolite from a contact metamorphic terrane, where the rate of heating is high relative to that in regional terranes, would show sector zoning.

Model III. This model is a special case of Model II. It assumes disequilibrium between the bulk of each sector and the matrix but chemical equilibrium between the surface layers of the sectors and the matrix. The chemical differences of the different sectors are assumed to be preserved, totally or partially, by growth if sector-zoning is observed. If staurolite crystals are found that are not sector-zoned, but have the same morphology of sector-zoned staurolite, another process must be incorporated into the model. This process is assumed to be one involving diffusion of ions out of the inner layers, in a direction perpendicular to the surface, in response to a tendency for the bulk of each sector to achieve equilibrium with the matrix and therefore with the other sectors. The thickness of the surface layer is assumed, in this model, to be as thick as the diameter of a cation polyhedron. The diffusion can be expressed as the jump time for a given ion to leave its position in the structure, leaving a hole which is available for filling by a different ion energetically more stable in the structure. The farther the ion in question is from the surface, the larger the jump time will be because, in a dense structure, the jump of an ion implies a vacancy for it to go into which must also be created by a jump. Thus, the length of time that a surface layer (first) of the crystal is exposed to the matrix will affect the degree to which the previous surface layer (second) approaches chemical equilibrium with the matrix, but the third layer will need a much longer period of time for further equilibration and its chemistry may be considered as being preserved by growth of the crystal. It is, of course, the chemistry of successive "third layers" which is measured by the electron microprobe.

The predictions of this model are (1) the partition of elements between sectors will be systematic and will be less pronounced in the outer portion than at the center of any single crystal because the length of time, according to the model, that a surface is exposed to the matrix increases as the crystal grows larger, (2) that the composition of a given sector at a given stage of growth will be the same for each crystal in a single hand specimen and for crystals of different specimens that have the same assemblage and that come from the same outcrop, and (3) staurolite from contact metamorphic terranes (rapidly heated) should show the phenomenon, and staurolite from regional terranes (slowly heated) should not show the phenomenon.

Model IV. This model is identical to Model III except that rather than

rate of crystal growth the presence of graphite would impede equilibration of the inner growth layers by blanketing the crystal surfaces. The presence of graphite must be considered as a possible diffusion-controlling factor because it is common to observe a shell of graphite around crystals of staurolite in graphite-bearing rocks. This shell of graphite is due to its exclusion from the volume occupied by the staurolite as the staurolite grows. Model IV presumes that the chemistry of the surface layer is determined during growth at a dislocation step and that graphite impedes equilibration of the surface layer, as well as the preceding surface layer, with the matrix by causing an increase of the jump time of ions out of the surface layer. The thickness of the surface layer, as defined in Model III, need not be as thick as the height of the dislocation step.

The predictions of Model IV are (1) sector-zoning would be dependent on the presence of graphite in the rock, and (2) sector-zoning would not be dependent on the geologic setting. Furthermore, the degree of partition from center to edge should be dependent on the amount of graphite in the rock. Thus, although all staurolite in one specimen should show similar partition effects, the partition should vary from rock to rock in one outcrop if the graphite/staurolite ratio varied; and it should be constant within single crystals.

Analytical Data

Staurolite of the Kwoiek Area, British Columbia. Figure 2 illustrates the results of total analyses, using an electron microprobe (Applied Research Laboratories, Model EMX), on twelve staurolite crystals from five specimens from one outcrop (station 350, Fig. 1, Hollister, 1969). Six of the crystals came from one specimen. One of these crystals was analyzed at six intervals outwards from the crystal center. The relative locations of these sections are shown in Figure 1. Photomicrographs of each of the six sections, cut nearly perpendicular to the *c*-axis, are shown in Figure 2 of Hollister and Bence (1967). Analyses of four sections of another crystal of the same specimen are also shown in Figure 2.

Analytical Procedure. Analyses were made for each of the three sectors of each polished section of a crystal, with the exception of the (010) sectors of sections 350F-1 and 350F-A-1. The (010) sectors were not large enough in these polished sections to obtain dependable results. There are, therefore, 58 complete analyses of staurolite represented in Figure 2.

The data were obtained in the following way: The analysis of the (010) sector of staurolite of 350F-D (Table 1) was used as a secondary standard. This analysis was obtained relative to kyanite (Si and Al), synthetic $MgSiO_3$ glass (Mg), synthetic fayalite (Fe), synthetic titaniferous diopside (Ti), zinc metal (Zn), and chemically analyzed hortonolite (Mn), using the correction procedure of Bence and Albee (1968). All data were corrected for drift, which was negligible, deadtime, and background. The two other analyses of Table 1 were made in the same manner. It is noted here that the analyses of Table 1 of Hollister and Bence (1967) are modified in Table 1 of this paper because they were made relative to an early set of the correction factors of the Bence and Albee (1968) scheme.

The remaining 57 analyses were obtained relative to the (010) sector of 350F-D. Each

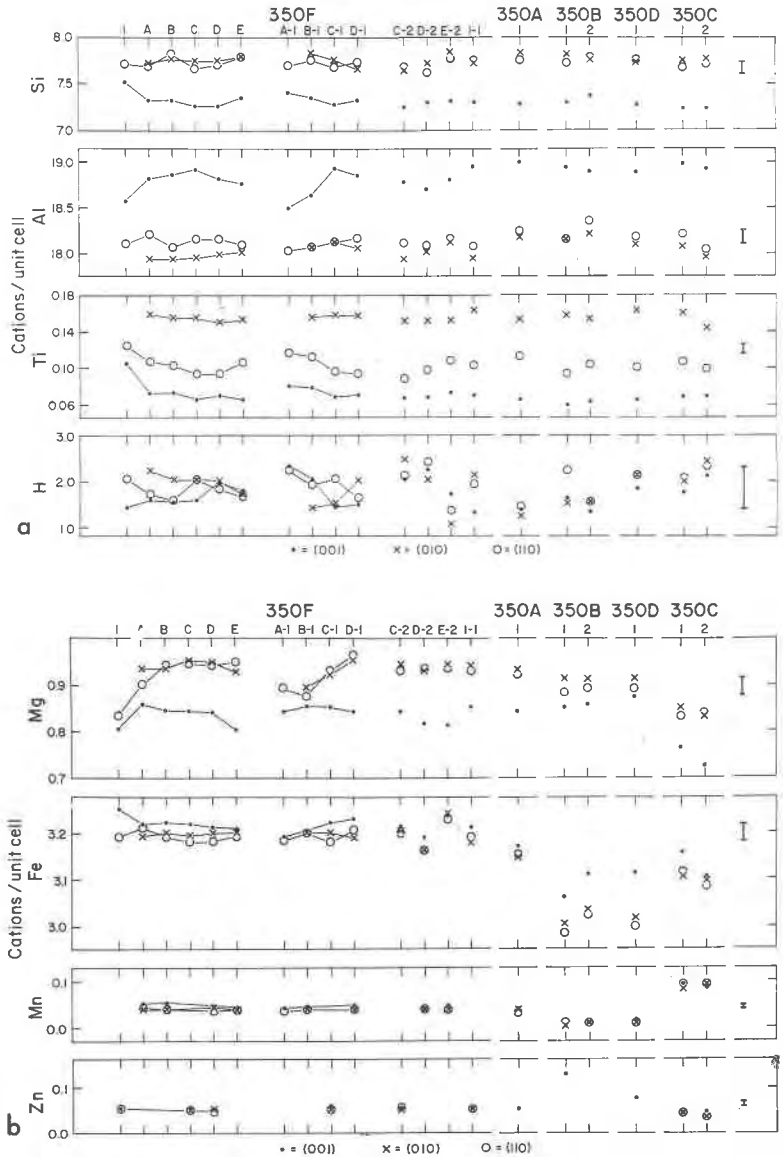

FIG. 2. Cation proportions, based on 48 oxygen to the unit cell, of 58 staurolite analyses in 20 polished sections from 5 rocks (350A-F). Analyses vertically arranged are from a single polished section. Except for grains in sections 350F-1 and 350A-1, there are three analyses to each crystal in each section, one each for the (001), (010), and (110) sectors. Analyses of successive sections of two single crystals are indicated by lines connecting analysis points. In both cases the extreme right hand points are closest to the center of the crystals. Error bars give standard deviations of each point, based on counting rate statistics. Zn and Mn were not determined in every crystal or sector.

TABLE 1. ANALYSES OF THE THREE SECTORS OF SPECIMEN 350F-D

Oxide	(001)		(010)		(110)	
SiO_2	25.63		27.53		27.58	
TiO_2	0.33		0.72		0.42	
Al_2O_3	56.83		54.30		54.69	
FeO	13.65		13.64		13.50	
ZnO	0.25		0.25		0.25	
MnO	0.21		0.18		0.18	
MgO	2.01		2.27		2.24	
H_2O	1.03		1.07		1.09	
Numbers of cations based on 48 oxygen						
Si	7.22	8.00	7.74	8.00	7.74	8.00
Al	0.78		0.26		0.26	
Al	18.10		17.73		17.84	
Ti	0.07	18.24	0.15	18.03	0.09	18.02
Mg	0.07		0.15		0.09	
Mg	0.77		0.80		0.85	
Fe	3.22	4.09	3.21	4.10	3.17	4.11
Mn	0.05		0.04		0.04	
Zn	0.05		0.05		0.05	
H	1.95		2.01		2.05	

Note: H_2O determined by subtraction; Fe assumed divalent and Ti assumed quadrivalent. See text for reasoning for site-occupancy assignments.

section was carbon-coated simultaneously with 350F-D and was analyzed immediately before and after the standard. In this way, no more than 20 minutes elapsed between analyses of the standard and any one of the unknowns. Extreme care was thus taken to correct for any drift in the instrument. Because the three sectors of the standard are so close in composition to any three sectors of the other sections of staurolite, deadtime was not a factor. Background readings were determined for each sector on each day of analysis.

Five separate points of each sector of each section of staurolite were analyzed. Repeat analyses of twenty seconds each were made at each analysis point. Reflected and transmitted light optics were used to be sure that the analysis point was not on a crack, pit, or near an inclusion. The analysis points on the (110) and (010) sectors were taken as near as possible to the boundaries with the (001) sector. Therefore, each set of three analyses belongs to the same growth stage of the staurolite. The beam diameter was 5–10 microns; sample current and accelerating voltage were 0.05 microamperes and 15 kilovolts.

Discussion of Results. As discussed in Hollister (1969), the assemblage chlorite-biotite-garnet-staurolite-plagioclase-ilmenite-quartz-graphite is trivariant, at a given pressure and temperature, in CaO, MnO, and ZnO. The constant Ti content of the (010) sectors in the staurolite of each of the five rocks (Fig. 2a) and the variable Mn and Zn content (Fig.

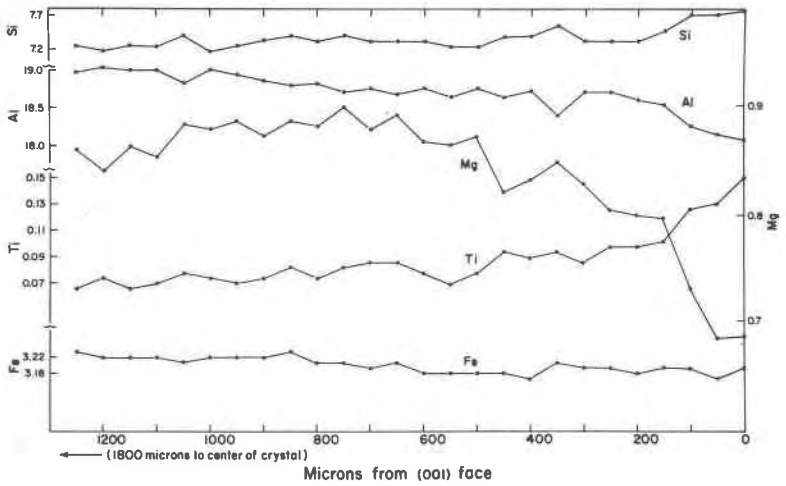

FIG. 3. Cation proportions along a transverse profile in the (001) sector of a crystal in section 350F-1. The crystal is homogeneous in the elements shown from the center to 1200 microns from the (001) face.

2b) between the staurolite of the five rocks suggests that Ti is not a compositional variable affecting the assemblage, as is expected from the presence of ilmenite in all five rocks, and that Mn and Zn are indeed possible compositional variables.

The outstanding chemical feature, other than the sector-zoning, shown in Figure 2 is the constancy of Zn, Mn, Fe, Al, Si, and Ti, within limits of error, for the (010) sectors of all staurolite crystals in a given specimen. The (010) sector is chosen for this comparison because, as noted in Fig. 3 of Hollister and Bence (1967), these elements are not zoned within the (010) sector. The variable Mg of all sectors, Ti of the (110) and (001) sectors, and Al and Si of the (001) sector are probably due to the continuous compositional variations within each sector. These continuous variations are illustrated in Figure 3, a profile along the *c*-axis within the (001) sector, and in Figure 3 of Hollister and Bence (1967).

The variation of elements between the staurolite of the different rocks reflects a mass balance effect. The more Mn or Zn in the structure, the less Mg and Fe. However, the mass balance effect is not quantitative, possibly because no suitable Zn standard was available when the analyses were made, thus indicating a possible systematic error in the Zn determination. The variations also reflect a nonideal effect of substitution of Mn on the Mg/Fe ratios in staurolite (Fig. 18 in Hollister, 1969).

The modal percentages of staurolite in the five rocks are: 350B, 2.5;

350C, 4.5; 350D, 5; 350A, 6.3; and 350F, 8.2 percent. There is no clear relation of abundance of staurolite to any compositional parameter, including Zn and Mn which are the only elements that vary significantly between the staurolites of the five specimens (Fe and Mg contents depend on the Zn and Mn contents).

The hydrogen contents of the sectors, calculated from the water content which was determined by subtracting the anhydrous totals from 100 percent, do not show significant variation either between sectors or between samples. Relative to the other cations, the error of the hydrogen content is, of course, quite large because it was not directly determined; but within the limits of the precision of the analyses, no case can be made for significant deviation from the ideal of two hydrogen ions to the unit cell. This result is in contrast to the conclusion of most authors who have made chemical analyses of staurolite (see Hietanen, 1969, for a recent reference to this problem).

The chemical characteristics of sector zoning are apparent in Figure 2. The (001) sectors differ from the (010) sectors in having higher Al, lower Si, lower Ti, lower Mg, and slightly higher Mn and Fe. The (110) sectors are similar to the (010) sectors except that they have lower Ti and slightly higher Al. The formulas shown in Table 1 for the three sectors of 350F-D illustrate the sectoral compositional variations in the individual sites. One can, of course, assign elements to sites in a manner different than that shown in Table 1; but the major difference between sectors cannot be obscured by juggling the data: there must be excess aluminum in both the tetrahedral and octahedral sites in the (001) sector. The suggestion in Table 1 of a coupled substitution of (Ti+Mg) for 2Al is discussed more fully in a later section.

Staurolite of Other Localities. Nineteen staurolite-bearing specimens from seventeen localities were studied to determine the occurrence and compositional characteristics of sector-zoned staurolite as a function of assemblage, graphite content, and style of metamorphism. Table 2 summarizes the results of this study.

It is clear from the results shown in Table 2 that (1) the phenomenon of sector-zoning is not unique to the Kwoiek area of British Columbia, (2) not all staurolite with the crystal form of the Kwoiek area specimens are sector-zoned, (3) staurolite of some localities are sector-zoned in Ti only, and (4) sector-zoning in staurolite is not restricted to a particular assemblage; it also occurs in rocks without graphite (#9 and #15) as well as with graphite.

Several interesting chemical characteristics of staurolite are also suggested by the data of Table 2. Zn and Mn show a large degree of vari-

TABLE 2. DATA ON STAUROLITE FROM SEVERAL LOCALITIES

Sample	Sector-zoned[a] in:				Analysis[b] of (010) sectors for:			Graphite content	Assemblage[d]							Notes	Locality
									ilmenite	muscovite	chlorite	biotite	garnet	aluminum silicate	iron oxide		
	Ti	Al	Si	Mg	Zn	Mn	Ti										
1	1.2	1.0	1.0	n.d.	0.5	0.1	0.6	Tr	×	×		×	×			e	Vermont, Dennis (1956) loc. A 2035
2	1.2	1.0	1.0	n.d.	0.4	0.1	0.6	Tr	×	×		×	×			e	Vermont, Dennis (1956) loc. A 2035
3	1.94	0.97	1.07	1.09	0.1	0.4	>0.7	Tr	×	×	×	×	×			e,l	Vermont, Hall (1959)
4	1.29	1.0	1.0	n.d.	0.6	>0.5	>0.7	Tr	×	×		×		fib.		e,f	Vermont, Hall (1959)
5	1.0	1.0	1.0	n.d.	0.3	0.5	0.7	1%	×	×		×		and.		e	Vermont, Woodland (1965) loc. B 1751
6	1.72	0.97	1.04	1.07	0.4	>0.5	0.4	Tr	×	×		×		and.		f	Vermont, Goodwin (1963) Page Hill
7	1.0	1.0	1.0	n.d.	n.d.	0.2	0.67	none	×	×	×	×	×			g	Vermont, Green (1963) ER 101
8	1.3	0.98	1.05	n.d.	n.d.	0.09	0.75	?	?	×	×	×	×			i	? Vermont, Green (1963) D-2
9	1.56	1.0	1.0	n.d.	0.2	0.1	0.4	none	×	×	×		×			j,m	Massachusetts, Zen and Hartshorn (1966) Lion's Head
10	1.19	1.0	1.0	n.d.	0.2	0.05	0.5	Tr	×	×	×	×	×			j	Massachusetts, Zen and Hartshorn (1966) ¾ mile SE of Lion's Head
11	1.0	1.0	1.0	n.d.	0.3	0.05	0.5	none	×	×		×			×	j	Ontario, Hounslow and Moore (1967) near Fernleigh
12	1.0	1.0	1.0	n.d.	0.3	0.2	0.6	none	×	×		×	×		×	g	Ontario, Hounslow and Moore (1967) near Fernleigh
13	1.2	1.0?	1.0?	n.d.	0.1	0.1	0.6	Tr	×	×		×	×			h	New Mexico, U.C.L.A. coll.
14	1.0	1.0	1.0	n.d.	0.1	0.3	0.5	Tr?	×	×	×	×				e	New Mexico, U.C.L.A. coll.
15	1.6	1.0?	1.0?	n.d.	0.2	0.3	0.6	none		×		×				i,m	Czechoslovakia, U.C.L.A. coll., Goldenstein
16	1.0	1.0	1.0	n.d.	0.4	>0.5	0.5	none	×	×			×		×	e	California, U.C.L.A. coll., Imperial Co.
17	1.0	1.0	1.0	n.d.	0.2	0.1	0.2	none	×	×	×	×	×			h	Tennessee, Ducktown
18	n.d.	n.d.	n.d.	n.d.	0.4	0.4	0.2	none	×			×	×		×	k	Unknown, Princeton coll.
19	1.0	1.0	1.0	n.d.	0.9	0.5	0.5	none		×					×	i	Brazil
20	2.18	0.955	1.074	1.131	0.25	0.18	0.72	½–2%[c]	×		×	×	×			f,m	Kwoiek area

ability from essentially none to 0.9 and 0.5 weight percent, respectively, whereas Ti is nearly constant in all except two specimens (#17 and #18). The staurolite with the lowest Ti content (#18) has a unique morphology, suggesting a possible relation of Ti content to morphology.

Origin of Sector Zoning

The chemical characteristics and occurrence of sector-zoned staurolite eliminate three of the proposed models on the origin of sector zoning. Model I (bulk chemical equilibrium) cannot hold because not all staurolite with the morphology of the type specimen are sector-zoned. Model IV (graphite impedes equilibration) is eliminated because the presence or absence of graphite does not correlate clearly with the presence or absence of sector-zoning. The model involving complete disequilibrium, Model II, does not appear to be correct because of the chemical systematics of the Kwoiek area staurolites. Model III (initial surface equilibrium) appears the most likely because (1) sector-zoning in the Kwoiek area staurolites shows chemical regularities which would not be expected in a complete disequilibrium situation and (2) not all staurolites are sector-zoned. It remains to be shown that all predictions of this model hold.

Figures 4 and 5 illustrate the "partitioning" of elements between the sectors as a function of percent of growth. The data shown in Figures 4 and 5 represent the bulk phase exchange partitioning inasmuch as no precise distribution data are available on crystallographic site populations. Fe and Mg are probably distributed in both octahedral and tetrahedral sites, and Al apparently varies in both the Si tetrahedral site as well as in the octahedral sites. Nevertheless, the ratios chosen are a func-

---

[a] Degree of sector-zoning given by factor element concentration in (010) sector exceeds element concentration in (001) sector. n.d., not determined.

[b] Concentration of elements in weight percent of oxide. Concentrations determined by comparing peak heights on wave-length profile scan with tissue of sample 350F-D.

[c] Estimated range of graphite content of five-specimens from outcrop 350.

[d] × denotes mineral present.

[e] (001) sector contains abundant graphite and/or quartz inclusions, rest of staurolite is free of inclusions.

[f] Inclusions along sector boundaries.

[g] Many quartz inclusions throughout staurolite.

[h] Sieve-textured, with many quartz inclusions.

[i] Extremely clean.

[j] Minor quartz and/or ilmenite inclusions.

[k] Has the forms (100), (010), (101).

[l] Associated with many granitic dikes.

[m] Pleochroic (010) sector.

tion of the variations between the sectors and are useful parameters to show the changes in the amount of sector-zoning with growth.

Figure 4 shows the "partitioning" of Fe and Mg between the (010) and (001) sectors to be nearly linear, with respect to percent of total growth, within the statistical counting rate uncertainty shown by the vertical bar. Additional points for the (110)/(001) ratio, near the 90 percent growth stage, are added to supplement the (010)/(001) data, because the (010) data are difficult to obtain at this stage of growth. The "partition" between about 0.91 near the staurolite center and 1.00 at the 100 percent staurolite growth stage shows that the cause of the difference in Mg and Fe between sectors diminishes in its effect as the staurolite becomes larger.

Figure 5 shows the "partitioning" of Al and Si between the (110) and (001) sectors. These data are shown without the (010) data because Ti, presumably substituting for Al in an octahedral site, zones in the same manner in the (110) and (001) sectors, whereas Ti is constant in the (010) sector. Thus, the true partition between the tetrahedral Si sites is approximated by considering total Al in the plot of Figure 5. The amount of Al actually substituting for Si is too small to determine accurately because of the large absorbtion of Si radiation by Al. The data are being stretched already to show the trends in both Figures 4 and 5, as is suggested by the large error bars. Nevertheless, there is a suggestion that the cause of the sectoral differences in Al and Si diminishes in its effect from a point near 60 percent of staurolite growth to the end of staurolite growth. There appears to be no change for the first 60 percent of growth.

The relation of Figures 4 and 5 can actually be deduced by examination of Figures 2 and 3. The data of Figure 2 show that Al and Si are nearly constant and equal within the (110) and (010) sectors, but Al is lower and Si is higher in these sectors relative to the (001) sector. The profiles of Figure 3 and points 350F-1, 350F-A-1, and 350-B-1 (Fig. 2) show that in the (001) sector Al decreases and Si increases to the (001) face, and the change begins at about the 60 percent growth stage.

The Ti content of the (110) and (001) sectors approaches that of the (010) sector with growth. This is apparent in Figs. 2 and 3 and illustrates that the cause of sector-zoning diminishes in effect in the site containing Ti, as well as in the tetrahedral sites occupied by Al and Si. Assuming Ti to be quadrivalent, the analyses of Table 1 and Figure 2, showing an inverse relation of Ti to Al, suggest that the Mg and Fe "partition" data shown in Figure 4 may actually be due in part to the effect of Ti substitution for Al, requiring for maintenance of charge balance further substitution of a divalent cation for Al. This substitution will be treated further in the next section.

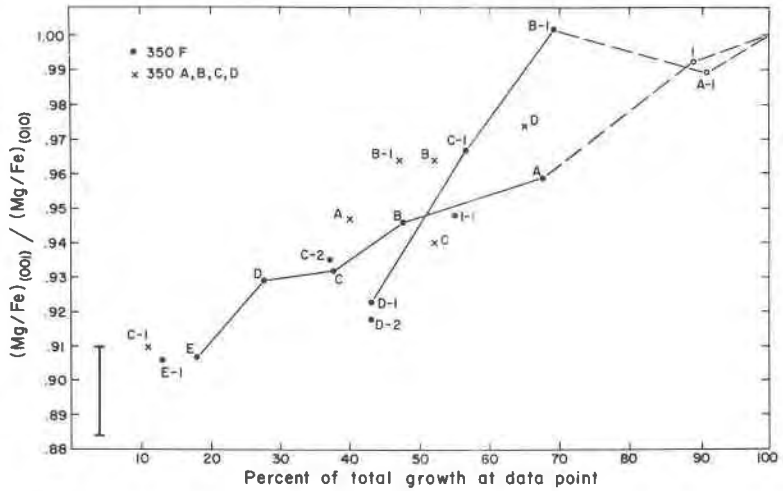

FIG. 4. Plot of "partitioning" of Mg and Fe between the (001) and (010) sectors of staurolite from the five specimens as a function of percent of growth. Lines connect data points of successive sections of two single crystals. Open circles are data points for the (001) and (110) sectors of two sections. Bar is standard deviation, based on counting-rate statistics for each point. "Percent of total growth" was determined by dividing the width of the (001) sector, measured along the *b*-axis direction, by the total width of the crystal, measured along the *b*-axis, and multiplying by 100 in both Figures 4 and 5.

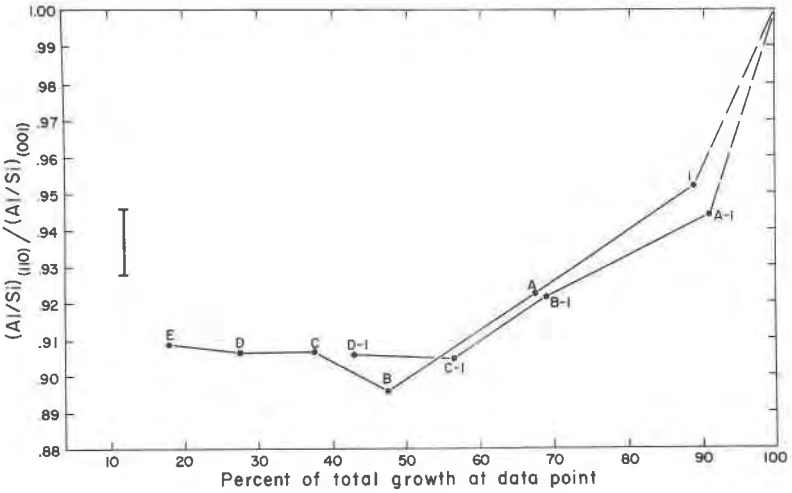

FIG. 5. Plot of "partitioning" of Si and Al between the (110) and (001) sectors of the two single crystals from specimen 350F-D as a function of growth. Bar is standard deviation, based on counting-rate statistics, for each point.

The decrease of magnitude of sector-zoning with growth is consistent with Model III (initial surface equilibrium), prediction (1). If a constant or decreasing flux of material to the growing staurolite is assumed, then the length of time that the staurolite surface (residence time) is exposed to the matrix increases with growth of the staurolite. If the jump time of ions out of the surface layer is of the order of the residence time, the jump time effect will become more and more important as the residence time of the staurolite surface decreases. A decreasing flux of material to the staurolite as it grows is probable because (1) staurolites of the Kwoiek area nucleated close to the maximum temperature (Hollister, 1969) each rock reached, implying growth under moderately super-saturated conditions and (2) garnets coexisting with the staurolites grew in a closed system, depleting the matrix in the constituents forming garnet (Hollister, 1966); other evidence indicates that staurolite must also grow according to a depletion model (Hollister, 1969, p. 2480).

The bulk partition of Mg and Fe between sectors begins to approach unity at an earlier stage of growth than the partition of Al and Si (Figs. 4 and 5). (Note: the bulk partition for any combination of elements between sectors must be unity when the sectors have the same composition.) This is permitted by Model III because the jump-times of different ions in the different sites would not be expected to be the same, unless a coupled substitution involving more than one site were involved. The data suggest that the rate of equilibration for the layer below the surface layer is greater for one set of atomic sites that it is for another.

If sector-zoning in staurolite is rate dependent and if jump-times vary significantly between sites, then the degree of chemical differences between sectors in staurolite would reflect the rate of heating of a rock. The occurrences of sector-zoned, partially sector-zoned, and non sector-zoned staurolites listed in Table 2 show that there is such a qualitative relationship. The Kwoiek area (a contact metamorphic terrane) shows sector-zoning of all elements in the staurolite; staurolites from high-level metamorphic terranes in northeastern Vermont (#3 and #6) are also sector-zoned in all elements, but to a lesser degree than the Kwoiek area specimens; staurolites from other terranes of northern New England (#1, #2, #4, #9, and #10) are sector-zoned in Ti only; and staurolites from a regionally metamorphosed terrane with widely spaced isograds near Fernleigh, Ontario (#11 and #12) are not sector-zoned at all.

In summary, all the evidence is consistent with Model III. The compositional regularities of the sector-zoned staurolites strongly point to near attainment of chemical equilibrium between growth surfaces. The

relation of the "partitioning" of elements between sectors to stage of growth and the occurrences in other localities of sector-zoned, partially sector-zoned, and non sector-zoned staurolites are consistent with the hypothesis that the rates of equilibration of the layer below the surface layer, which has a three-dimensional atomic environment, are on the order of the growth rates of the staurolites. Thus, depending on rates of growth of the crystal, the staurolites can show varying degrees of approach to three-dimensional chemical equilibrium. It remains to understand the details of the process of sector-zoning and to discuss in more detail the geologic consequences of the process.

Mechanism

Structure of Staurolite. Náray-Szabó and Sasvári (1958) determined the structure of staurolite and described it as being made up of kyanite-like layers alternating with layers containing Al in octahedral sites, Fe and Mg in tetrahedral sites, and hydrogen ions. The structure was refined and confirmed by Smith (1968), who identified another weakly occupied octahedral site between faces of the iron tetrahedra. The structure is monoclinic, but psuedo-orthorhomic with β near 90°. Monoclinic staurolite lacks the *c*-glide plane normal to the *a*-axis of orthorhombic staurolite. Dollase and Hollister (1969) have shown for the sector-zoned staurolite of the Kwoiek area that the symmetry of the (001) sector is orthohombic and that the symmetry of the (010) sector is monoclinic. This difference in structure was tentatively interpreted to be a result of ordered aluminum in the partially filled chain of edge-sharing octahedra called the Al(3) octahedra (Smith, 1968) in the monoclinic case and of disordered aluminum in the Al(3) octahedra in the orthorhombic case.

Assumptions Used for Assignment of Site Preferences. In the discussion of the chemical substitution in staurolite which follows, it will be assumed that the chemistry of the kyanite-like part of the staurolite structure is pure Al_2SiO_5. Very small amounts of Fe and Ti would be expected to be the only impurities (Chinner, *et al.*, 1969; Albee and Chodos, 1969) in this part of the structure.

A structural comparison of staurolite with the spinel hercynite can also be made. The iron and silicon tetrahedra and the aluminum octahedra of part of the staurolite structure (Fig. 7) have the same arrangement and position as the iron tetrahedra and aluminum octahedra in hercynite. The structural similarity of hercynite and staurolite, applicable to the layer in staurolite containing tetrahedral iron atoms, forms a basis of a second chemical assumption. This assumption is that the element site preferences in staurolite in the iron-bearing layer will

approximate that in the normal spinels, reported by Navrotsky and Kleppa (1967). Given octahedral and tetrahedral sites, the order of preference for the tetrahedral site is: Zn^{2+}, Mn^{2+}, Fe^{3+}, $Mg^{2+} = Fe^{2+}$, Al^{3+}, and Ti^{4+} (other elements considered by Navrotsky and Kleppa, but not important in the staurolite, are omitted). Thus, in staurolite, Zn and Mn are assigned to the tetrahedral site, Al^{3+} and Ti^{4+} to the octahedral site, and Mg and Fe are assigned predominately to the tetrahedral site.

This model of site preference is consistent with the chemical data of the sector-zoned staurolites. In Figure 2, a reciprocal relation of Ti for Al between the (110) and (010) sectors suggests that Ti and Al share an octahedral site. The sector-zoning of Mg between the (001) and (010) sectors in the same direction as Ti, and without equivalent sector zoning in Fe, Zn, or Mn, suggests that Mg substitutes for Al in a coupled substitution with Ti. This implies that Mg has a stronger preference for the octahedral site than the other divalent cations, and it implies that Ti is predominently quadrivalent, as assumed earlier. It is concluded that these data indicate the coupled substitution (Mg+Ti) for 2Al.

Iron will be assumed to be divalent in the Kwoiek-area staurolite. This assumption (Hollister, 1969) is based on the observation that no ferric-iron bearing oxide is present in the Kwoiek-area rocks and that the staurolites of the Kwoiek area coexist with graphite and ilmenite, as association indicative of low fugacity of oxygen.

The site assignments in Table 1 reflect the above assumptions. Zn, Mn, Fe, and Mg are in the ferromagnesian tetrahedral site, Al and Ti are in the octahedral sites, and an amount of Mg equivalent to the Ti content is assigned to an octahedral site. Sufficient aluminum is assigned to the silicon site to completely fill that position.

Surface Structure of Staurolite. Figure 6 illustrates the atomic configuration on the (010) face of staurolite at a level which passes through the centers of the tetrahedral, predominantly iron-bearing sites. The position of atoms was taken from Smith (1968). The Al(3A) octahedral and the tetrahedral sites of Smith are shown as occupied polyhedra. The Al(3B), U(1), and U(2) sites are shown as unoccupied. The oxygen (1B) atoms, shared by the tetrahedra and the unoccupied Al(3B) octahedra, each have a $(-1/2)$ residual charge, and it is presumed that the hydrogen ions of staurolite are in the neighborhood of the Al(3B) position.

Figure 7 shows the atomic configuration of the (001) face at a level which passes through the occupied Al(3A) positions of Figure 6. Also shown are the traces of two possible (110) faces where they intersect the (001) face.

The important differences between the (001) and (010) faces are: (1)

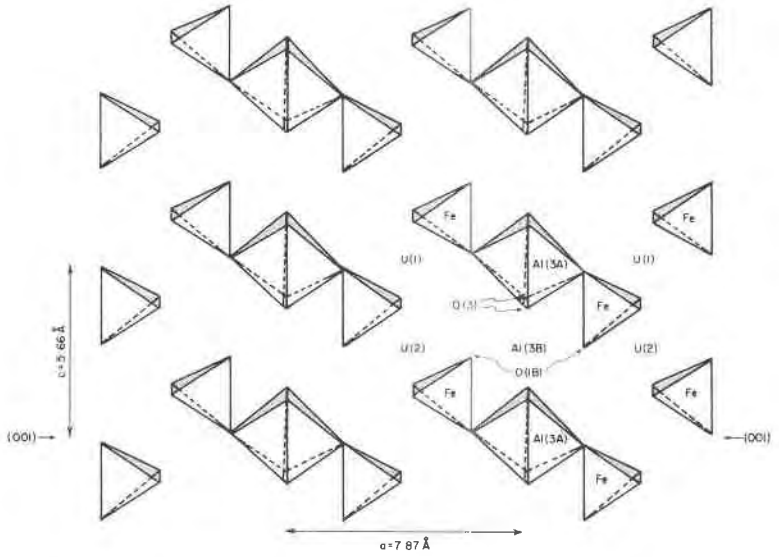

FIG. 6. Arrangement of Al(3) octahedra, Fe tetrahedra, and weakly occupied U octahedra (Smith, 1968) on the (010) face, as viewed at a slightly oblique angle. Cell edges and positions of atoms from Smith (1968). Trace of plane of (001) projection (Fig. 7) on (010) face is indicated.

the silicon tetrahedra lie nearly in the same plane as the iron tetrahedra on (001), Figure 7, but are behind the Al(3A) and Al(3B) octahedra of the (010) face shown in Figure 6 and (2) *in the plane* of (001) the centers of the nearest Al(3) octahedra (Fig. 7) are 10 angstroms apart, whereas *in the plane* of (010) the Al(3A) and Al(3B) octahedra share edges in a continuous chain. These two major differences are exploited in the following discussions.

Mechanism of Al-Si Sector Variations. Consider atom by atom accretion on the faces as a mechanism of staurolite growth, and consider that the tetrahedral positions on the (010) face (Fig. 6) are filled, but the Al(3) positions are not. An Al atom impinging on the surface will settle in one of the Al(3) positions. Whichever position it settles in can be defined as an Al(3A) position. The next Al atom impinging on the same row parallel to the *c*-axis can settle in a neighboring Al(3B) or an Al(3A) position. If it settles in the Al(3B) position, it will not only create a situation involving shared edges between octahedra but would also require a negative charge excess of $(-1/2)$ on the oxygen atom labelled O(3) on Fig. 6. However, because the charge on this oxygen is fully satisfied by the initial addition of an Al atom, the second Al atom would

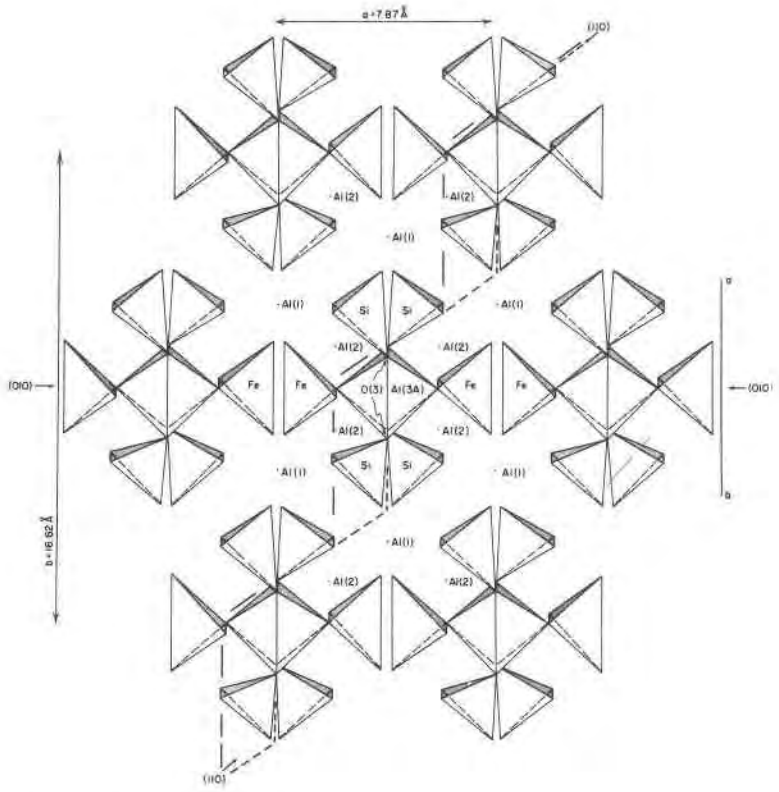

FIG. 7. Arrangement of Al(3) octahedra, Al(1) and Al(2) octahedra, and Si and Fe tetrahedra on the (001) face, as viewed at a slightly oblique angle. Cell edges and positions of atoms from Smith (1968). Trace of plane of (010) projection (Fig. 6) on (001) face is indicated; also, two possible traces of (110) face are indicated. Line a b shows that portion of staurolite structure equivalent to the hercynite structure.

most probably move from the unfavorable Al(3B) site into the more favorable Al(3A) site. A continuation of this process will develop a chain of Al(3) octahedra alternately occupied by Al atoms and, presumably, hydrogen ions to maintain local charge balance.

The parallel chain of Al(3) octahedra, one a-cell dimension from the first, must fill with Al and H atoms in the same manner to give a configuration similar to that shown in Figure 6 because any other regular configuration will lead to either orthorhombic symmetry or monoclinic symmetry with twice the observed *b*- and *a*-cell dimensions. The next layer added to the one shown in Figure 6 will be a part of the kyanite structure, presumably without significant chemical irregularities. Continuing build-up of the crystal on the (010) face will lead to nearly ideal

staurolite, chemically and structurally, with the formula $Fe_4Al_{18}Si_8O_{48}H_2$ and its symmetry monoclinic, as observed (Dollase and Hollister, 1969).

The (001) surface presents the interesting possibilities for chemical variance. Consider a layer as shown in Figure 7 as already formed. An impinging Al atom has available to it the Al(3B) *and* the two tetrahedral silicon sites which connect at the corners of the shared edge of the Al (3A) and Al (3B) octahedra at the O(3) atoms. If it settles in an Al(3B) site, a potential excess charge of (-1) will be needed on both the O(3) atoms; but this excess charge can be eliminated by 2Al instead of 2Si going into the connecting tetrahedral sites. Thus, a fault can occur in the (001) sector which is not ideally possible in the (010) sector. The coupled substitution at the fault is 3Al for $(2Si + H)$; for each extra Al in the Al(3) sites of the (001) sector over the (010) sector, there will be two extra Al ions substituting for Si.

This pattern of substitution can be very irregular; it need not occur at the same growth stage in adjacent chains of Al(3) positions, and it need not occur at regular intervals within a single chain of Al(3) positions. The pattern of aluminum and hydrogen ions in the Al(3) sites will be completely disordered, in contrast with the Al of the (010) sector, and the symmetry of the (001) sector will be orthorhombic, as observed (Dollase and Hollister, 1969), because disorder of Al in the Al(3) sites adds as an additional symmetry element the *c*-glide.

The formulas in Table 1 show, for the (001) sector relative to the (010) sector, 0.52 atoms excess tetrahedral Al and 0.37 atoms excess octahedral Al. These results are encouraging in that they show the right amount of excess Al in the two sites of the (001) sector predicted by the proposed coupled substitution on the (001) surface; given the errors on the analyses, better agreement with prediction is not expected. Furthermore, (Mg+Ti) should probably be considered with Al in the substitutions in the Al(3) site. Matching the number of Ti atoms with Mg atoms, as is done in Table 1, gives the differences in total occupancy of the Al(3) sites between the two sectors as 0.21 atoms. The analyses also suggest fewer hydrogen ions in the (001) sector, but this difference has little significance in light of the large error in the indirect determination of the water content.

The similarity of Al and Si contents in the (110) and (010) sectors is expected because the (110) crystal faces are also parallel to the Al(3) chains of octahedra, making implausible the occurrence of two Al(3) octahedra sharing an edge.

Mechanism of Sector-zoning of Ti. The mechanism proposed for the sector-zoning of Ti between the (010) and (001) sectors is based on the same principles used to discuss the sector-zoning of Si and Al. The assumptions

are that Ti is predominately quadrivalent and that it substitutes with Mg for octahedrally coordinated aluminum, as discussed above. On the (010) face, in which the Al(3) chains can lie (Fig. 6), the substitution of (Ti+Mg) for 2Al can occur simultaneously, whereas on the (001) face (Fig. 7), only one Al(3) site of a single chain is available at any stage of growth so that either a Ti or a Mg ion will produce charge imbalances that cannot be neutralized until the next layer is added. Local charge balance can be achieved on the (010) face if the Al(3B) site between the Mg and Ti ions remains vacant and two hydrogen ions enter the structure in the vicinity of the Al(3B) site between the Mg ion and the next Al ion in Al(3A).

As the length of time that the surface is exposed to the matrix increases, the equal partition between the bulk of the two sectors and the matrix of the rock external to the staurolite should lead to the same Ti content in each sector. The partition of Ti between the (010) surface and the matrix should be the closest to the bulk partition because the entire length of the Al(3) positions is exposed to the matrix at any one time; therefore, Ti, according to Model III, would be expected to be constant in (010) and to increase with growth in (001) as it does (Fig. 3).

The sector-zoning of Ti between the (010) and (110) sectors is not understood, nor is the reason why the (010) sector is more highly pleochroic than the (110) or (001) sectors (Hollister and Bence, 1967). It may be that these two phenomena are related.

Mg and Fe Variations. The phenomenon of sector zoning of Ti, Al, and Si is fairly well documented; but it is far from conclusive that there is any differential occupancy of the ferromagnesian tetrahedral site in the various sectors. The Mg/Fe data of Figure 4 do not prove occupancy differences in this site because most, if not all, of the relation shown could be due to changing Mg content in the Al(3) sites in the (001) sector as a result of an increasing, with growth, content of Ti in the (001) sector, as discussed above.

Consequences

Summary of Mechanism of Sector-zoning. The mechanism of creating different compositions on different growth surfaces involves equilibration of the surface layer, probably only one cation polyhedron thick, with the matrix. The degree of equilibration will be dependent primarily on the atomic configuration of the thin surface layer. Different compositions will be approached if the atomic configurations of different surface layers are markedly different. When the next growth layer is added, the former

surface layer will have more of a three-dimensional atomic configuration and will be nearly equivalent to the former (first) surface layers of the other sectors. Thus, any re-equilibration through the (second) surface layer will lead to similar compositions of the inner (first) layers of the different sectors. The inner (first) layer will have opportunity to re-equilibrate with the matrix as vacancies develop in the (second) surface layer during the process of surface re-equilibration. The whole process of re-equilibration will be rate dependent; and, if the next (third) surface layer is added at a faster rate than this rate of re-equilibration, the original (first) layer may never reach complete equilibrium because the probability of two vacancies remaining open simultaneously above the first layer will be very small.

An Origin of Order-disorder in Crystals. The mechanism proposed for the origin of sector-zoning suggests one possible mechanism for developing disorder in a crystal. The orthorhombic symmetry of the (001) sector and monoclinic symmetry of the (010) sector implies that, at least for staurolite, the apparent disorder is a product of crystal growth and not due solely to either temperature of crystallization or rate of cooling. The suggestion is that rate of growth, combined with a favorable surface configuration of cation sites, can be a factor in producing disorder in a crystal.

The difference in symmetry between the sectors of staurolite correlates with a difference in chemistry. The sector with excess Al is orthorhombic, with Al presumably disordered in the partially filled Al(3) site. It is not known if sectoral differences in symmetry can ever exist without a chemical difference. A possible example of sectoral differences in symmetry without a chemical difference may be adularia (Chaisson, 1950, p. 541–2, 545). Adularia should be studied in more detail to see if the apparent sectoral differences in symmetry correlate with sectoral differences in composition.

Other minerals known to be sector-zoned in the major constituents are andalusite (Hollister and Bence, 1967), titanaugite (Preston, 1966; Smith and Carmichael, 1969; Strong, 1969; and Hollister and Hargraves, 1970), and possibly tourmaline (Donnay, 1968). Chloritoid with an inclusion-free hour-glass structure (see Halferdahl, 1961, p. 134) should be examined for compositional sector-zoning; and it may be that the polymorphism in chloritoid (Halferdahl, 1961, p. 65–83) is related to the sector-zoning phenomenon. It is probable that the number of examples of sector-zoning and sectoral differences in crystal symmetry will increase as more attention is given the sector-zoning phenomenon.

Mechanism of the Nucleation Process and a Possible Mechanism of Prefererd Orientation of Crystals. The phenomenon of sector-zoning emphasizes the importance of surfaces in the determination of the chemistry of a crystal. It also suggests that the composition of a surface layer is not necessarily preserved with growth because of the exchange of ions between the surface and the matrix. The implication of this process for nucleation in a solid medium is that a surface of one mineral, by exchange at the surface, can become a nucleating surface of another mineral. Given the driving force of a negative change of free energy of a reaction, a surface of one mineral could develop, by exchange of cations, the chemistry of another without substantial reorganization of the anions. Once the new chemistry is developed, the new mineral in the rock could proceed to grow on the reorganized surface of the old. The activation energy for the nucleation would be expressed as a function of the number of bonds of the surface of the seed mineral that must be broken in the exchange process. This model of nucleation is similar to one discussed by De Vore (1956).

The phenomenon of sector-zoning may offer a mechanism for the development of preferred orientation of crystals. The densest *surface* of a potentially sector-zoned crystal will be stable at a slightly lower temperature than any other surface of the crystal, and, therefore, in a slowly heated rock it will be the nucleus layer. The nucleus layer will most likely form on the plane of a seed crystal whose anion arrangement is closest to that of the densest surface of the new crystal. If the anion layer of the seed crystal is less dense than that of the dense layer of the new crystal, those planes of the seed crystal most nearly perpendicular to the principal stress direction will be favored as nucleation sites. If the anion layer of the seed crystal is denser than the dense layer of the new crystal, the opposite geometry will hold. Once nucleated, the new crystal would continue to grow with the original, preferred orientation of the nucleus.

This mechanism for the development of preferred orientation of crystals is consistent with the general observation that preferred orientation is most common in regional metamorphic rocks as compared with contact metamorphic rocks. Rapid heating at the contact of a crystallizing magmatic pluton provides opportunity for a considerable overstepping of reaction temperatures (Hollister, 1969, p. 2492) so that at the temperature of nucleation the probability for developing one orientation in preference to another would be relatively small: all orientations of a crystal would be stable if the reaction temperature were overstepped prior to nucleation. In a regional metamorphic terrane the rate of heating is presumably slow enough so that the temperature at which nucleation takes place can be close to that of the reaction temperature for only one surface

within a crystal. This would enhance the probability for crystal growth to take place from a single, preferred orientation of the plane in which nucleation takes place.

Acknowledgements

This research was supported by National Science Foundation Grant GA 1503 while the author was at UCLA and by the Higgins Fund of Princeton University. I thank Y. Kolodny (UCLA) and M. Semet (UCLA) for assistance in obtaining the data in Table 2 and H. Adams (UCLA) for assistance in the computer programing and reduction of data. The computational facilities were provided by the UCLA Campus Computing Network. Discussions with W. A. Dollase and W. G. Ernst (UCLA), H. D. Holland (Princeton), and W. B. Kamb (Caltech) contributed to the content of this paper. I gratefully thank A. L. Albee (Caltech), W. A. Dollase, H. D. Holland, W. B. Kamb, J. V. Smith (University of Chicago), and D. R. Waldbaum (Harvard) for their comments on the manuscript; but all inadequacies and errors are mine. Staurolite samples were obtained through the courtesy of E. Olsen (Field Museum of Natural History), J. Moore (Carleton University, Ontario), J. Green (University of Minnesota, Duluth), D. Barker (University of Texas, Austin), and E-an Zen (U. S. Geological Survey). Other samples were collected by the author while accompanying A. L. Albee in the field of Vermont. I thank him and his family for their hospitality during that visit.

References

Albee, A. L., and A. A. Chodos (1969) Minor element content of coexistent Al_2SiO_5 polymorphs. *Amer. J. Sci.* **267,** 310–316.

Barton, P. B., Jr., P. M. Bethke, and P. Toulmin, 3rd (1963) Equilibrium in ore deposits. *Mineral. Soc. Amer. Spec. Paper* **1,** 171–185.

Bence, A. E., and A. L. Albee (1968) Empirical correction factors for the electron microanalysis of silicates and oxides. *J. Geol.* **76,** 382–403.

Chaisson, Ursula (1950) The optics of triclinic adularia. *J. Geol.* **58,** 537–547.

Chinner, G. A., J. V. Smith, and C. R. Knowles (1969) Transition-metal contents of Al_2SiO_5 polymorphs. *Amer. J. Sci.* **267-A,** *Schairer vol.*, 96–113.

Cohen, A. J. (1960) Substitutional and interstitial aluminum impurity in quartz, structure and color center interrelationships. *J. Phys. Chem. Solids,* **13,** 321–325.

Dennis, J. G. (1956) The geology of the Lyndonville area, Vermont. *Vt. Geol. Surv., Bull.* **8,** 98 pp.

Devore, G. W. (1956) Surface chemistry as a chemical control on mineral association. *J. Geol.* **64,** 31–55.

Dollase, W. A., and L. S. Hollister (1969) X-ray evidence of ordering differences between sectors of a single staurolite crystal. *Geol. Soc. Amer., Atlantic City Meet. Progr.*

Donnay, G. (1968) Crystalline heterogeneity, evidence from electron probe study of Brazilian tourmaline. *Carnegie Inst. Wash. Year Book,* **67,** 219–20.

Goodwin, B. K. (1963) Geology of the Island Pond area, Vermont. *Vt. Geol. Surv., Bull.* **20,** 111 pp.

Halferdahl, L. B. (1961) Chloritoid: Its composition, x-ray and optical properties, stability, and occurrence. *J. Petrology,* **2,** 49–135.

Hall, L. M. (1959) The geology of the St. Johnsbury quadrangle, Vermont and New Hampshire. *Vt. Geol. Surv., Bull.* **13,** 105 pp.

Harker, A. (1939) *Metamorphism.* Methuen: London. 2nd ed. 362 p.

HIETANEN, A. (1969) Distribution of Fe and Mg between garnet, staurolite, and biotite in aluminum-rich schist in various metamorphic zones north of the Idaho batholith. *Amer. J. Sci.* **267,** 422–456.

HOLLISTER, L. S. (1966) Garnet zoning: an interpretation based on the Rayleigh fractionation model. *Science,* **154,** 1647–1651.

——— (1967) Sector zoning in staurolite, Kwoiek area, British Columbia. *Can. Mineral.* **9,** 292–293.

——— (1968) Compositional characteristics of sector-zoned staurolite. *Trans. Amer. Geophys. Union,* **49,** 345–346.

——— (1969) Contact metamorphism in the Kwoiek area of British Columbia: an end member of the metamorphic process. *Geol. Soc. Amer. Bull.* **80,** 2465–2494.

——— AND R. B. HARGRAVES (1970) Compositional zoning and its significance in pyroxenes from two course-grained Apollo 11 samples. *Geochim. Cosmochim. Acta, Apollo 11 Vol.,* (in press).

——— AND A. E. BENCE (1967) Staurolite: sectoral compositional variations. *Science,* **158,** 1053–1056.

HOUNSLOW, A. W., AND J. M. MOORE, JR. (1967) Chemical petrology of Grenville schists near Fernleigh, Ontario. *J. Petrology,* **8,** 1–28.

KINSMAN, D. J. J., AND H. D. HOLLAND (1969) The co-precipitation of cations with $CaCO_3$–IV. The co-precipitation of Sr^{+2} with aragonite between 16° and 96°C. *Geochim. Cosmochim. Acta,* **33,** 1–17.

MCINTIRE, W. L. (1963) Trace element partition coefficients—a review of theory and applications to geology. *Geochim. Cosmochim. Acta,* **27,** 1209–1265.

NÁRAY-SZABÓ, I., AND K. SASVÁRI (1958) On the structure of staurolite, $HFe_2Al_9Si_4O_{24}$. *Acta Crystallogr.* **11,** 862–865.

NAVROTSKY, A., AND O. J. KLEPPA (1967) The thermodynamics of cation distributions in simple spinels. *J. Inorg. Nucl. Chem.* **29,** 2701–1714.

PENFIELD, S. L., AND J. H. PRATT (1894) On the chemical composition of staurolite, and the regular arrangement of its carbonaceous inclusions. *Amer. J. Sci.* **47,** 81–89.

PRESTON, J., 1966. An unusual hourglass structure in augite. *Amer. Mineral.* **51,** 1227–1233.

RAMBERG, H., AND G. W. DEVORE (1951) The distribution of Fe and Mg in coexisting olivines and pyroxenes. *J. Geol.* **59,** 193–210.

SMITH, A. L., AND I. S. E. CARMICHAEL (1969) Quaternary trachy basalts from southeastern California. *Amer. Mineral.* **54,** 909–923.

SMITH, J. V. (1968) The crystal structure of staurolite. *Amer. Mineral.* **53,** 1139–1155.

STRONG, D. F. (1969) Formation of the hour-glass structure in augite. *Mineral. Mag.* **37,** 472–479.

TORGESON, J. L. (1966) Purification by single-crystal growth. Ann. N. Y. Acad. Sci. **137,** 30–43.

WOODLAND, B. G. (1965) The geology of the Burke quadrangle, Vermont. *Vt. Geol. Surv., Bull.* **28,** 151 pp.

ZEN, E-AN, AND J. H. HARTSHORN (1966) Geologic map of The Bashbish Falls quadrangle, Mass., Conn., and New York. *U. S. Geol. Surv. Quadrangle Map* GQ-570.

Manuscript received, November 4, 1969; accepted for publication, February 17, 1970.